Pergamon

Int. J. Solids Structures Vol. 35, No. 20, pp. 2639–2653, 1998

0020–7683/98 $19.00 + .00

PII: S0020–7683(97)00191–1

THERMOMECHANICAL BUCKLING OF DELAMINATED COMPOSITE LAMINATES

WAN-LEE YIN
School of Civil Environmental Engineering, Georgia Institute of Technology, Atlanta, Georgia, U.S.A.

(*Received* 3 *November* 1996; *in revised form* 20 *June* 1997)

Abstract—A thermomechanical buckling analysis of multilayered laminates with (across-the-width) strip delaminations is conducted on the basis of anisotropic thermoelasticity of the constituent layers and the Kirchhoff–Love hypothesis of the classical laminate theory. With the assumption of generalized plane deformation, the present analysis yields *exact*, closed-form solutions of the delamination model under in-plane compression and shear loads and a temperature load that may vary arbitrarily in the thickness direction. A characteristic equation is obtained for the thermal and mechanical load parameters associated with the states of bifurcation. This equation reveals *explicitly* the effects of various geometrical, material and load parameters on the buckling of the delaminated plate. The solutions of the characteristic equation indicate that a moderate temperature gradient in the thickness direction may drastically reduce the axial bifurcation load. © 1998 Elsevier Science Ltd. All rights reserved.

NOMENCLATURE

x, y, z	Cartesian coordinates referred to the center of the laminate
z_c	position of the middle surface of a sublaminate
$z' \equiv z - z_c$	thickness coordinate referred to the middle plane of a sublaminate
$\sigma_{\beta\gamma}$ $(\beta, \gamma = 1, 2)$	in-plane components of the stress
$\varepsilon_{\beta\gamma}$ $(\beta, \gamma = 1, 2)$	in-plane components of the strain
$T(z)$	temperature load
T_u, T_l	temperature on the top and bottom surfaces of the laminate

Notations for k*th layer of the laminate*

$h_k \equiv z_k - z_{k-1} = z'_k - z'_{k-1}$	thickness
$g'_k \equiv (z'^2_k - z'^2_{k-1})/2$	$f_k \equiv (z'^3_k - z'^3_{k-1})/3$
$a^{(k)}_{ij}$ $(i, j = 1, 2, 6)$	in-plane anisotropic elastic compliance
$\mathbf{Q}^{(k)} \equiv [a^{(k)}_{ij}]^{-1}$	in-plane stiffness matrix
$\alpha^{(k)}_{\beta\gamma}$ $(\beta, \gamma = 1, 2)$	in-plane thermal expansion coefficients

Notations for the sublaminates

$t, H, h \equiv t - H$	thickness of the intact and disbonded sublaminates
$\mathbf{A} \equiv \Sigma h_k \mathbf{Q}^{(k)} = [A_{ij}]$	extensional stiffness matrix
$\mathbf{B} \equiv -\Sigma g'_k \mathbf{Q}^{(k)} = [B_{ij}]$	bending–extension coupling matrix
$\mathbf{D} \equiv \Sigma f'_k \mathbf{Q}^{(k)} = [D_{ij}]$	bending and twisting stiffness matrix
$[\underline{A}_{ij}]$, $[\underline{B}_{ij}]$, $[\underline{D}_{ij}]$	stiffness matrices of the lower disbonded sublaminate
$[\bar{A}_{ij}]$, $[\bar{B}_{ij}]$, $[\bar{D}_{ij}]$	stiffness matrices of the upper disbonded sublaminate
Δ, $\underline{\Delta}$, $\bar{\Delta}$	sublaminate properties defined by eqns (20) (25), etc.
D, $\underline{D}$, $\bar{D}$	sublaminate properties defined by eqns (19), (24), etc.
$\varepsilon^0_{\beta\gamma}$, $\underline{\varepsilon}^0_{\gamma}$, $\bar{\varepsilon}^0_{\beta\gamma}$	middle plane strains
$\kappa_{\beta\gamma}$, $\underline{\kappa}_{\beta\gamma}$, $\bar{\kappa}_{\beta\gamma}$	middle plane curvatures
$N_{\beta\gamma}$, $\underline{N}_{\beta\gamma}$, $\bar{N}_{\beta\gamma}$	in-plane normal and shearing forces
$M_{\beta\gamma}$, $\underline{M}_{\beta\gamma}$, $\bar{M}_{\beta\gamma}$	bending and twisting moments
$N^*_{\beta\gamma}$, $\underline{N}^*_{\beta\gamma}$, $\bar{N}^*_{\beta\gamma}$	thermal forces
$M^*_{\beta\gamma}$, $\underline{M}^*_{\beta\gamma}$, $\bar{M}^*_{\beta\gamma}$	thermal moments
w, $\underline{w}$, $\bar{w}$	deflections
$\varepsilon, \gamma, \xi, \eta, \kappa$	deformation parameters of the intact sublaminate [eqn (13a)]
$\underline{\varepsilon}, \underline{\gamma}, \underline{\xi}, \underline{\eta}, \lambda$	deformation parameters of the lower laminate [eqn (13b)]
$\bar{\varepsilon}, \bar{\gamma}, \bar{\xi}, \bar{\eta}, \mu$	deformation parameters of the upper sublaminate [eqn (13c)]
A	amplitude of deflection [eqn (9)]
$2L$, $2a$	length of the laminate and of the delamination
$b \equiv L - a,\ \beta \equiv \varepsilon_y,\ S \equiv N_{xy},$	$P \equiv -N_x = D(\kappa t)^2,\ \underline{P} \equiv -\underline{N}_x = \underline{D}(\lambda t)^2,\ \bar{P} \equiv -\bar{N}_x = \bar{D}(\mu t)^2$
P_{cr}	critical value of P
$\mathscr{P} \equiv P_{cr}(L/t)^2/(\pi^2 D)$	normalized axial buckling load
$\theta \equiv (t/a) A \kappa \sin \kappa b$	nondimensionalized amplitude of deflection
ν, α	Poisson ratio and thermal expansion coefficient of an isotropic layer.

1. INTRODUCTION

In the past decade, considerable research efforts have been expended on the buckling and postbuckling behavior of composite beams and plates with internal delaminations (Simitses *et al.*, 1985; Wang *et al.*, 1985; Yin *et al.*, 1986; Garg, 1988; Kardomateas and Schmueser, 1988; Yin and Fei, 1988; Storakers, 1989; Whitcomb, 1989; Yin, 1989; Yin and Jane, 1992; Chai, 1990; Chen, 1991; Larsson, 1991; Cochelin and Potier-Ferry, 1991; Peck and Springer, 1991; Hutchinson and Suo, 1992; Lee *et al.*, 1993). Although hygrothermal loads, in addition to mechanical loads, may aggravate the instability of delaminated composite structures, such effects have not been systematically studied. Skin panels in high-speed flight structures may be subjected to a significant temperature gradient. A thin delaminated layer on the hot surface of the panel is particularly liable to the initiation of local buckling. Generally speaking, the effect of temperature load on the stability of delaminated structures depends on many factors, including the anisotropic elastic and thermal properties of the successive layers of the laminate, the size and location of the delamination, and combined mechanical and thermal loads. An understanding of such complex dependence of the stability characteristic of the delaminated structure upon multifarious factors cannot be gained from a small number of elaborate numerical solutions. It requires efficient, versatile analysis methods applicable to various delamination models covering a wide range of geometrical, material and loading parameters.

A postbuckling analysis of one-dimensional delamination models with general multilayered configuration was given previously without considering the thermal loads (Yin, 1986). Closed-form analytical solutions of the anisotropic delamination model were obtained based on von Karman's nonlinear strain–displacement relation. It was found that initial buckling and postbuckling deformation of the model may be considerably influenced by certain effects peculiar to anisotropic laminates, including bending–stretching coupling and shear–extension coupling. An outstanding feature of these generalized plane deformation solutions is that, due to bending–stretching coupling, the axial and shearing components of the membrane strain depend sinusoidally on the axial coordinate, even though the axial force and the in-plane shearing force are constant in each (intact or disbonded) sublaminate.

In the present work, we study thermomechanical buckling of delaminated composite laminates subjected to a temperature field that may vary arbitrarily in the thickness direction, $T = T(z)$. It is shown that the effects of the temperature load are *completely* characterized by three effective thermal forces: $\underline{N}_x^*$ and $\bar{N}_x^*$ in the lower and upper disbonded sublaminates and N_{xy}^* in the intact sublaminate. When these constant effective forces are combined with the corresponding mechanical forces, the thermal buckling problem of the strip delamination model assumes a mathematical form identical to the stability problem under purely mechanical loads. The thermal and mechanical load parameters associated with the bifurcation states are determined by a sytsem of three algebraic equations, eqns (34)–(36), which may be reduced to a single characteristic equation after eliminating the parameters λ and μ. The characteristic equation reveals *explicitly* how the various geometrical, material and loading parameters affect the buckling behavior of the delamination model. Such relations are not easily discerned from numerical solutions using three-dimensional finite element analysis. In this work, the characteristic equation is solved for homogeneous isotropic models and laminated anisotropic models with various delamination lengths. The results indicate that a temperature gradient in the thickness direction may drastically change the axial buckling load.

The analysis of the present paper is *exact* within the context of the classical laminated plate theory. General anisotropic thermoelastic constitutive equations are used to model the intact and disbonded sublaminates, so that the resulting buckling solutions show the coupling of in-plane axial, transverse and shearing deformations (in contrast to previous works on isotropic and specially orthotropic delamination models which do not manifest such coupling effects). Furthermore, since a moisture gradient causes nonuniform swelling in the same way that a temperature gradient causes differential thermal expansion, the effect of moisture on the buckling of delaminated plates may be determined by the present analysis when its concentration and expansion coefficients are substituted for the temperature and thermal expansion coefficients.

2. THERMOELASTIC CONSTITUTIVE EQUATIONS OF AN ANISOTROPIC LAMINATE

The analysis of thermal buckling of a delaminated composite laminate requires a concise formulation of the thermoelastic constitutive equations of intact and disbonded sublaminates. In each sublaminate, the membrane strains and the moment resultants are usually referred to the middle surface of the sublaminate. On the other hand, the temperature field is described as a function of global coordinates (x, y, z), where $z = 0$ is the middle surface of the *intact* sublaminate in the delamination model. Hence, in considering the disbonded sublaminates, it is convenient to use, in addition to (x, y, z), another system of coordinates (x, y, z') such that $z = z' + z_c$, where z_c is the position of the middle surface of the (upper or lower) disbonded sublaminate relative to that of the intact sublaminate.

Each sublaminate may consist of a number of homogeneous, orthotropic elastic layers with different orientation angles and possibly made of different materials. The layers are separated by parallel interfaces at $z = z_k$ (or, equivalently, $z' = z'_k \equiv z_k - z_c$). The layers and their interfaces are numbered successively from the bottom of the sublaminate to the top, so that the kth layer is bounded below by the $(k-1)$th interface and bounded above by the kth interface. In the kth layer, the in-plane strain components ε_x, ε_y and γ_{xy} are related to the in-plane stresses and the temperature field T in the following manner:

$$\begin{Bmatrix} \varepsilon_x \\ \varepsilon_y \\ \gamma_{xy} \end{Bmatrix} = \begin{bmatrix} a_{11}^{(k)} & a_{12}^{(k)} & a_{16}^{(k)} \\ a_{12}^{(k)} & a_{22}^{(k)} & a_{26}^{(k)} \\ a_{16}^{(k)} & a_{26}^{(k)} & a_{36}^{(k)} \end{bmatrix} \begin{Bmatrix} \sigma_x \\ \sigma_y \\ \tau_{xy} \end{Bmatrix} + T \begin{Bmatrix} \alpha_x^{(k)} \\ \alpha_y^{(k)} \\ \alpha_{xy}^{(k)} \end{Bmatrix} \tag{1}$$

where the matrix $[a_{ij}^{(k)}]$ characterizes the elastic compliance of the anisotropic layer and $\alpha_x^{(k)}$, $\alpha_y^{(k)}$ and $\alpha_{xy}^{(k)}$ denote the in-plane thermal expansion coefficients.

According to the Kirchhoff–Love assumption for classical laminates, the values of ε_x, ε_y and γ_{xy} at a distance z' from the midplane are determined by the mid-plane strains and curvatures ε_x^0, ε_y^0, γ_{xy}^0, κ_x, κ_y and κ_{xy} of the sublaminate:

$$\varepsilon_x = \varepsilon_x^0 - z'\kappa_x, \quad \varepsilon_y = \varepsilon_y^0 - z'\kappa_y, \quad \gamma_{xy} = \gamma_{xy}^0 - z'\kappa_{xy} \tag{2}$$

We assume that the temperature field varies only in the thickness direction, $T = T(z)$. Substituting eqn (2) into eqn (1), we obtain

$$\begin{Bmatrix} \sigma_x \\ \sigma_y \\ \tau_{xy} \end{Bmatrix} - \mathbf{Q}^{(k)} \left(\begin{Bmatrix} \varepsilon_x^0 \\ \varepsilon_y^0 \\ \gamma_{xy}^0 \end{Bmatrix} - z' \begin{Bmatrix} \kappa_x \\ \kappa_y \\ \kappa_{xy} \end{Bmatrix} \right) = -T(z)\mathbf{Q}^{(k)} \begin{Bmatrix} \alpha_x^{(k)} \\ \alpha_y^{(k)} \\ \alpha_{xy}^{(k)} \end{Bmatrix} \tag{3}$$

where $\mathbf{Q}^{(k)}$ stands for the inverse matrix of the 3×3 symmetric matrix in eqn (1). Integrating the in-plane stress components and their first moments across the thickness of the successive layers and summing the results over all layers of the sublaminate, one obtains the stress and moment resultants

$$N_x = \int \sigma_x \, dz, \quad N_y = \int \sigma_y \, dz, \quad N_{xy} = \int \tau_{xy} \, dz, \tag{4a}$$

$$M_x = -\int z'\sigma_x \, dz, \quad M_y = -\int z'\sigma_y \, dz, \quad M_{xy} = -\int z'\tau_{xy} \, dz \tag{4b}$$

If σ_x, σ_y and τ_{xy} on the right-hand side of the preceding expressions are replaced, respectively, by the first, second and third elements of the right-hand side of eqn (3), one obtains, instead, the thermal forces N_x^*, N_y^*, N_{xy}^* and the thermal moments M_x^*, M_y^* and M_{xy}^*. They stand for the force and moment resultants that would result from the temperature load $T(z)$ in the hypothetical state when the sublaminate is constrained to have vanishing total strain. Notice that when the temperature load depends only on the thickness coordinate, the thermal forces and thermal moments are *constant* in the sublaminate.

In the kth layer, we define $h_k = z_k - z_{k-1}$ and

$$g_k = (z_k^2 - z_{k-1}^2)/2, \quad f_k = (z_k^3 - z_{k-1}^3)/3$$

$$g'_k = (z'^2_k - z'^2_{k-1})/2, \quad f'_k = (z'^3_k - z'^3_{k-1})/3 \tag{5}$$

$$\mathbf{A} = \Sigma h_k \mathbf{Q}^{(k)}, \quad \mathbf{B} = -\Sigma g'_k \mathbf{Q}^{(k)}, \quad \mathbf{D} = \Sigma f'_k \mathbf{Q}^{(k)} \tag{6}$$

The three symmetric matrices **A**, **B** and **D** characterize, respectively, the stiffness properties of the sublaminate associated with extension, extension–bending coupling and bending. Consistent with the notation of eqn (1), the elements of these matrices have the indices ranging over 1, 2 and 6.

Equations (2)–(6), along with the definitions of the thermal forces and thermal moments, yield the thermoelastic constitutive equation of the sublaminate:

$$\begin{Bmatrix} N_x - N_x^* \\ N_y - N_y^* \\ N_{xy} - N_{xy}^* \\ M_x - M_x^* \\ M_y - M_y^* \\ M_{xy} - M_{xy}^* \end{Bmatrix} = \begin{bmatrix} \mathbf{A} & \mathbf{B} \\ \mathbf{B} & \mathbf{D} \end{bmatrix} \begin{Bmatrix} \varepsilon_x^0 \\ \varepsilon_y^0 \\ \gamma_{xy}^0 \\ \kappa_x \\ \kappa_y \\ \kappa_{xy} \end{Bmatrix} \tag{7}$$

3. GENERALIZED PLANE DEFORMATION OF THE STRIP DELAMINATION MODEL

Consider a laminated beam-plate of thickness t and axial length $2L$ containing an across-the-width delamination of length $2a$ at a depth h beneath the upper surface (Fig. 1). The delamination is assumed to be located symmetrically with respect to the two clamped ends of the laminate. Let $[A_{ij}]$, $[B_{ij}]$ and $[D_{ij}]$ denote the stiffness matrices of the intact segment. Furthermore, let $[\underline{A}_{ij}]$, $[\underline{B}_{ij}]$ and $[\underline{D}_{ij}]$ stand for the corresponding matrices of the lower delaminated sublaminate, and $[\bar{A}_{ij}]$, $[\bar{B}_{ij}]$ and $[\bar{D}_{ij}]$ those of the upper delaminated sublaminate. With $H = t - h$, the following equalities are easily established:

$$A_{ij} = \underline{A}_{ij} + \bar{A}_{ij}, \quad B_{ij} = \underline{B}_{ij} + \bar{B}_{ij} + \underline{A}_{ij}h/2 - \bar{A}_{ij}H/2,$$

$$D_{ij} = \underline{D}_{ij} + \bar{D}_{ij} + \underline{B}_{ij}h - \bar{B}_{ij}H + \underline{A}_{ij}h^2/4 + \bar{A}_{ij}H^2/4 \tag{8}$$

In generalized plane-strain buckling, the three sublaminates in the right half of the delaminated plate undergo transverse deflections of the following forms.

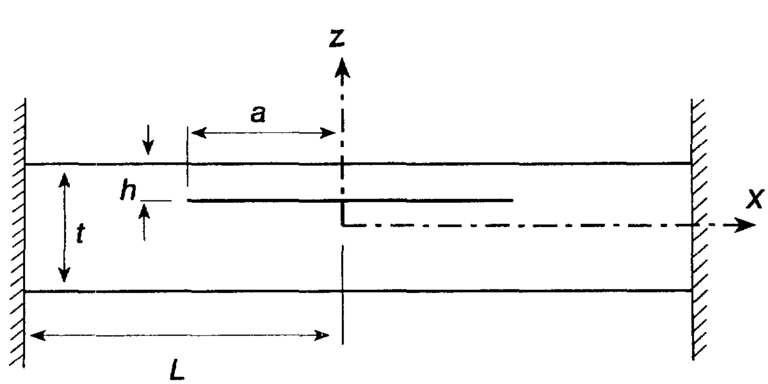

Fig. 1. One-dimensional delamination model.

$$w(x) = A\{\cos\kappa(L-x)-1\}, \quad (a \leqslant x \leqslant L) \tag{9a}$$

$$\underline{w}(x) = A\{(\kappa\sin\kappa b/\lambda\sin\lambda a)(\cos\lambda a-\cos\lambda x)+\cos\kappa b-1\}, \quad (0 \leqslant x \leqslant a) \tag{9b}$$

$$\bar{w}(x) = A\{(\kappa\sin\kappa b/\mu\sin\mu a)(\cos\mu a-\cos\mu x)+\cos\kappa b-1\}, \quad (0 \leqslant x \leqslant a) \tag{9c}$$

where A, κ, λ and μ are constants yet to be determined, $b \equiv L-a$, and x denotes the axial coordinate measured from the midpoint of the beam-plate. These expressions satisfy the continuity of deflection and slope at the crack tip, $w(a) = \underline{w}(a) = \bar{w}(a)$ and $w'(a) = \underline{w}'(a) = \bar{w}'(a)$, the symmetry conditions at the midpoint, $\underline{w}'(0) = \bar{w}'(0) = 0$, as well as the clamped end condition, $w(L) = 0$ and $w'(L) = 0$. The curvatures of the sublaminates are obtained by differentiating eqn (9) twice:

$$\kappa_x = -(\theta/t)(\kappa a/\sin\kappa b)\cos\kappa(L-x), \quad \kappa_y = \kappa_{xy} = 0 \tag{10a}$$

$$\underline{\kappa}_x = (\theta/t)(\lambda a/\sin\lambda a)\cos\lambda x, \quad \underline{\kappa}_y = \underline{\kappa}_{xy} = 0 \tag{10b}$$

$$\bar{\kappa}_x = (\theta/t)(\mu a/\sin\mu a)\cos\mu x, \quad \bar{\kappa}_y = \bar{\kappa}_{xy} = 0 \tag{10c}$$

where

$$\theta \equiv (t/a)A\kappa\sin\kappa b. \tag{11}$$

Furthermore, the middle plane strains that satisfy the compatibility conditions

$$\partial^2\gamma_{xy}^0/(\partial x\,\partial y) = \partial^2\varepsilon_x^0/\partial_y^2+\partial^2\varepsilon_y^0/\partial_x^2$$

(with similar conditions for the disbonded sublaminates) are given by

$$\varepsilon_y^0 = \underline{\varepsilon}_y^0 = \bar{\varepsilon}_y^0 = \beta, \tag{12}$$

$$\varepsilon_x^0 = \varepsilon+\xi\cos\kappa(L-x), \quad \gamma_{xy}^0 = \gamma+\eta\cos\kappa(L-x), \quad (a \leqslant x \leqslant L) \tag{13a}$$

$$\underline{\varepsilon}_x^0 = \underline{\varepsilon}+\underline{\xi}\cos\lambda x, \quad \underline{\gamma}_{xy}^0 = \underline{\gamma}+\underline{\eta}\cos\lambda x, \quad (0 \leqslant x \leqslant a) \tag{13b}$$

$$\bar{\varepsilon}_x^0 = \bar{\varepsilon}+\bar{\xi}\cos\mu x, \quad \bar{\gamma}_{xy}^0 = \bar{\gamma}+\bar{\eta}\cos\mu x, \quad (0 \leqslant x \leqslant a) \tag{13c}$$

where β, ε, $\underline{\varepsilon}$, $\bar{\varepsilon}$, γ, $\underline{\gamma}$, $\bar{\gamma}$, ξ, $\underline{\xi}$, $\bar{\xi}$, η, $\underline{\eta}$ and $\bar{\eta}$ are additional constant which, together with κ, λ, μ and θ (or A), completely characterize the generalized plane deformation of the delamination model.

The strain field given by eqns (12) and [13(a–c)] generalizes that given in Yin *et al.* (1986) for a homogeneous beam plate by adding terms that vary sinusoidally with the axial coordinate. Such terms arise in cases of laminated beam because the curvature κ_x varies sinusoidally and because there is coupling between bending and in-plane deformation for general unsymmetric laminates.

The thermoelastic constitutive equation of the two disbonded sublaminates are similar in form to eqn (7). The thermal forces of the disbonded sublaminates may be obtained by integrating the right-hand side of eqn (3) and summing the results over the group of layers in each sublaminate. It is easily verified that, when the temperature field depends only on z, the thermal forces of the disbonded sublaminates are related to those of the intact sublaminate by the additivity relation

$$N_{\alpha\beta}^* = \underline{N}_{\alpha\beta}^*+\bar{N}_{\alpha\beta}^*, \quad (\alpha, \beta = 1, 2) \tag{14}$$

Furthermore, the thermal moments are related by

$$-M^*_{\alpha\beta}+M^*_{\alpha\beta}+\bar{M}^*_{\alpha\beta}+\underline{N}^*_{\alpha\beta}h/2-\bar{N}^*_{\alpha\beta}H/2=0,\quad (\alpha,\beta=1,2) \tag{15}$$

Notice that the preceding relations among the thermal forces and thermal moments of the sublaminates are formally identical to those among the stiffness matrices in the first two equations of eqn (8).

Substituting eqns (9)–(13) and the thermoelastic constitutive relation, eqn (7), into the equilibrium equations

$$N_{x,x}+N_{xy,y}=0,\quad N_{xy,x}+N_{y,y}=0, \tag{16a, b}$$

$$M_{x,xx}+2M_{xy,xy}+M_{y,yy}-N_xw_{,xx}-2N_{xy}w_{,xy}-N_yw_{,yy}=0 \tag{16c}$$

(where the commas indicate partial differentiation), one obtains

$$A_{11}\xi+A_{16}\eta-B_{11}A\kappa^2=0,\quad A_{16}\xi+A_{66}\eta-B_{16}A\kappa^2=0, \tag{17a, b}$$

$$B_{11}\xi+B_{16}\eta-D_{11}A\kappa^2-N_xA=0, \tag{17c}$$

$$N_x-N^*_x=A_{11}\varepsilon+A_{12}\beta+A_{16}\gamma,\quad N_{xy}-N^*_{xy}=A_{16}\varepsilon+A_{26}\beta+A_{66}\gamma, \tag{17d, e}$$

$$M_x-M^*_x=B_{11}\varepsilon+B_{12}\beta+B_{16}\gamma-D\theta t(\kappa a/\sin\kappa b)\cos\kappa(L-x) \tag{17f}$$

Furthermore, by substituting eqns (9a), (17f) and (11) into eqn (16c), one finds that the *compressive* axial force in the laminate is directly proportional to κ^2:

$$P\equiv -N_x=D(\kappa t)^2 \tag{18}$$

where

$$D\equiv(1/\Delta)\begin{vmatrix} A_{11} & A_{16} & B_{11}/t \\ A_{16} & A_{66} & B_{16}/t \\ B_{11}/t & B_{16}/t & D_{11}/t^2 \end{vmatrix} \tag{19}$$

$$\Delta\equiv A_{11}A_{66}-(A_{16})^2 \tag{20}$$

Equations [16(a, b)] also imply that the two deformation parameters ξ and η in eqn (13a) may be expressed in terms of κ and θ:

$$\xi=(1/\Delta)(A_{66}B_{11}/t-A_{16}B_{16}/t)\theta\kappa a/(\sin\kappa b) \tag{21a}$$

$$\eta=(1/\Delta)(A_{11}B_{16}/t-A_{16}B_{11}/t)\theta\kappa a/(\sin\kappa b) \tag{21b}$$

Similar results may be obtained for the disbonded sublaminates from the corresponding equilibrium and constitutive equations. Thus, for the lower sublaminate we have

$$\underline{N}_x-\underline{N}^*_x=\underline{A}_{11}\underline{\varepsilon}+\underline{A}_{12}\beta+\underline{A}_{16}\gamma,\quad \underline{N}_{xy}-\underline{N}^*_{xy}=\underline{A}_{16}\underline{\varepsilon}+\underline{A}_{26}\beta+\underline{A}_{66}\underline{\gamma} \tag{22a, b}$$

$$\underline{M}_x-\underline{M}^*_x=\underline{B}_{11}\underline{\varepsilon}+\underline{B}_{12}\beta+\underline{B}_{16}\gamma+\underline{D}\theta t(\lambda a/\sin\lambda a)\cos\lambda x \tag{22c}$$

where

$$\underline{P}\equiv -\underline{N}_x=\underline{D}(\lambda t)^2 \tag{23}$$

$$\underline{D}\equiv(1/\underline{\Delta})\begin{vmatrix} \underline{A}_{11} & \underline{A}_{16} & \underline{B}_{11}/t \\ \underline{A}_{16} & \underline{A}_{66} & \underline{B}_{16}/t \\ \underline{B}_{11}/t & \underline{B}_{16}/t & \underline{D}_{11}/t^2 \end{vmatrix} \tag{24}$$

$$\underline{\Delta} \equiv \underline{A}_{11}\underline{A}_{66} - (\underline{A}_{16})^2 \tag{25}$$

Furthermore, eqns (21a, b) have their counterparts

$$-\underline{\xi} = (1/\underline{\Delta})(\underline{A}_{66}\underline{B}_{11}/t - \underline{A}_{16}\underline{B}_{16}/t)\theta\lambda a/(\sin\lambda a) \tag{26}$$

$$-\underline{\eta} = (1/\underline{\Delta})(\underline{A}_{11}\underline{B}_{16}/t - \underline{A}_{16}\underline{B}_{11}/t)\theta\lambda a/(\sin\lambda a) \tag{27}$$

The corresponding results for the upper sublaminate are obvious. In particular,

$$\bar{P} \equiv -\bar{N}_x = \bar{D}(\mu t)^2 \tag{28}$$

where $\bar{D}$ and $\bar{\Delta}$ are defined by expressions analogous to eqns (24) and (25).

4. BIFURCATION STATES AND THE CHARACTERISTIC EQUATION

As mentioned previous, eqns [9(a–c)] ensure continuity of the deflection and the slope at the crack tip. The continuity condition of the transverse in-plane displacement v may be obtained by integrating the shearing strains $\underline{\gamma}_{xy}$ and $\bar{\gamma}_{xy}$ of eqns (13b, c). This yields

$$\underline{\gamma} + \underline{\eta}(\sin\lambda a)/(\lambda a) = \bar{\gamma} + \bar{\eta}(\sin\mu a)/(\mu a)$$

or,

$$\underline{\gamma} - \bar{\gamma} = \theta\{(1/\underline{\Delta})(\underline{A}_{11}\underline{B}_{16}/t - \underline{A}_{16}\underline{B}_{11}/t) - (1/\bar{\Delta})(\bar{A}_{11}\bar{B}_{16}/t - \bar{A}_{16}\bar{B}_{11}/t)\} \tag{29}$$

Continuity of the axial displacement u at the crack tip requires that $-\bar{u}(a) = \underline{u}(a) + (t/2)w'(a)$, where

$$-\bar{u}(a) = -\int_0^a \bar{\varepsilon}_x^0 \,\mathrm{d}x + \int_0^a \{\bar{w}'(x)\}^2 \,\mathrm{d}x$$

$$-\underline{u}(a) = -\int_0^a \underline{\varepsilon}_x^0 \,\mathrm{d}x + \int_0^a \{\underline{w}'(x)\}^2 \,\mathrm{d}x$$

In considering bifurcation of the delamination model from membrane states to buckled states, one may restrict attention to infinitesimally small deflections so that the second integrals in the expressions of $\bar{u}(a)$ and $\underline{u}(a)$ may be neglected. Hence the continuity condition yields

$$\underline{\varepsilon} - \bar{\varepsilon} = \theta\{1/2 - (1/\underline{\Delta})(\underline{A}_{16}\underline{B}_{16}/t - \underline{A}_{66}\underline{B}_{11}/t) + (1/\bar{\Delta})(\bar{A}_{16}\bar{B}_{16}/t - \bar{A}_{66}\bar{B}_{11}/t)\} \tag{30}$$

In view of eqn (8), the balance conditions of the in-plane forces

$$N_x = \underline{N}_x + \bar{N}_x, \quad N_{xy} = \underline{N}_{xy} + \bar{N}_{xy}$$

and similar relations for the thermal forces [eqn (14)] yield

$$-A_{11}\varepsilon - A_{16}\gamma + \underline{A}_{11}\underline{\varepsilon} + \underline{A}_{16}\underline{\gamma} + \bar{A}_{11}\bar{\varepsilon} + \bar{A}_{16}\bar{\gamma} = 0$$

$$-A_{16}\varepsilon - A_{66}\gamma + \underline{A}_{16}\underline{\varepsilon} + \underline{A}_{66}\underline{\gamma} + \bar{A}_{16}\bar{\varepsilon} + \bar{A}_{66}\bar{\gamma} = 0$$

These results follow from eqns [17(d), (e)] for the intact sublaminate, eqns [22(a, b)] for the lower disbonded sublaminate, and similar equations for the upper sublaminate. Using eqn (8) again, we obtain from the above

$$\underline{A}_{11}(\underline{\varepsilon}-\varepsilon)+\underline{A}_{16}(\underline{\gamma}-\gamma)+\bar{A}_{11}(\bar{\varepsilon}-\varepsilon)+\bar{A}_{16}(\bar{\gamma}-\gamma) = 0 \tag{31}$$

$$\underline{A}_{16}(\underline{\varepsilon}-\varepsilon)+\underline{A}_{66}(\underline{\gamma}-\gamma)+\bar{A}_{16}(\bar{\varepsilon}-\varepsilon)+\bar{A}_{66}(\bar{\gamma}-\gamma) = 0 \tag{32}$$

Furthermore, by evaluating eqns (17f), (22c) and a similar equation for the upper sublaminate at $x = a$, and by using the moment balance condition at the crack tip,

$$-M_x+\underline{M}_x+\bar{M}_x+\underline{N}_x h/2-\bar{N}_x H/2 = 0$$

along with a similar equation for the thermal forces and moments [eqn (15)], we obtain

$$\begin{aligned}&(\underline{B}_{11}+\underline{A}_{11}h/2)(\underline{\varepsilon}-\varepsilon)+(\underline{B}_{16}+\underline{A}_{16}h/2)(\underline{\gamma}-\gamma)\\&+(\bar{B}_{11}-\bar{A}_{11}H/2)(\bar{\varepsilon}-\varepsilon)+(\bar{B}_{16}-\bar{A}_{16}H/2)(\bar{\gamma}-\gamma)\\&+(D\kappa a\,\mathrm{ctn}\,\kappa b+\underline{D}\lambda a\,\mathrm{ctn}\,\lambda a+\bar{D}\mu a\,\mathrm{ctn}\,\mu a)\theta t = 0\end{aligned} \tag{33}$$

Equations (29)–(33) constitute a system of five linear homogeneous equations for the five unknowns $\underline{\varepsilon}-\varepsilon$, $\underline{\gamma}-\gamma$, $\bar{\varepsilon}-\varepsilon$, $\bar{\gamma}-\gamma$ and θ. The system has a nontrivial solution if and only if the determinant of the coefficient matrix vanishes. This condition yields the following equation:

$$\begin{aligned}&-\Delta(D\kappa a\,\mathrm{ctn}\,\kappa b+\underline{D}\lambda a\,\mathrm{ctn}\,\lambda a+\bar{D}a\,\mathrm{ctn}\,a)\\&+\Gamma_1\{(\underline{A}_{11}\underline{B}_{16}/t-\underline{A}_{16}\underline{B}_{11}/t)\underline{\Delta}-(\bar{A}_{11}\bar{B}_{16}/t-\bar{A}_{16}\bar{B}_{11}/t)/\bar{\Delta}\}\\&+\Gamma_2\{-(\underline{A}_{16}\underline{B}_{16}/t-\underline{A}_{66}\underline{B}_{11}/t)/\underline{\Delta})+(\underline{A}_{16}\underline{B}_{16}/t-\bar{A}_{66}\bar{B}_{11}/t)/\bar{\Delta}\} = 0\end{aligned} \tag{34}$$

where

$$\Gamma_1 \equiv \begin{vmatrix} A_{11} & A_{16} & B_{11}/t \\ A_{16} & A_{66} & B_{16}/t \\ \bar{A}_{16} & \bar{A}_{66} & (\bar{B}_{16}-\bar{A}_{16}H/2)/t \end{vmatrix}, \quad \Gamma_2 \equiv \begin{vmatrix} A_{11} & A_{16} & B_{11}/t \\ A_{16} & A_{66} & B_{16}/t \\ \bar{A}_{11} & \bar{A}_{66} & (\bar{B}_{11}-\bar{A}_{11}H/2)/t \end{vmatrix}$$

It is remarkable that eqn (34), the result of the preceding lengthy analysis, is utterly independent of the thermal load and involves only the parameters κ, λ and μ (corresponding to the axial compression forces in the sublaminates). Another relation among the same set of parameters may be obtained by substituting eqns (18), (23) and (28) into the balance condition of axial forces, $N_x = \underline{N}_x+\bar{N}_x$. This yields

$$D(\kappa t)^2 = \underline{D}(\lambda t)^2+\bar{D}(\mu t)^2 \tag{35}$$

The bifurcation states are characterized by eqns (34), (35) and an additional equation which, unlike the preceding equations, does depend on the thermal load. To obtain this equation, we notice that, in the states associated with and prior to bifurcation, the entire delamination model is subjected to a uniform strain with $\varepsilon_x = \varepsilon$, $\varepsilon_y = \beta$ and $\gamma_{xy} = \gamma$. The moment balance condition

$$-M_x+\underline{M}_x+\bar{M}_x+\underline{N}_x h/2-\bar{N}_x H/2 = 0$$

in conjunction with eqns (8) and (15) and the sublaminate constitutive equations yields

$$\langle A_{11}\rangle\varepsilon+\langle A_{12}\rangle\beta+\langle A_{16}\rangle\gamma = -\langle P+N_x^*\rangle$$

where, for any parameter Φ defined in both disbonded sublaminates, the symbol $\langle\ \rangle$ denotes

$$\langle\Phi\rangle \equiv (\bar{\Phi}H-\underline{\Phi}h)/(2t)$$

By eliminating ε and γ from the last equation and the constitutive equations of the laminate

$$A_{11}\varepsilon+A_{12}\beta+A_{16}\gamma = -P-N_x^*,\quad A_{16}\varepsilon+A_{26}\beta+A_{66}\gamma = S-N_{xy}^*$$

we obtain

$$\begin{vmatrix}\underline{A}_{11} & A_{16}\\ \underline{A}_{16} & A_{66}\end{vmatrix}(\bar{D}\mu^2t^2+\bar{N}_x^*)/2-\begin{vmatrix}\bar{A}_{11} & A_{16}\\ \bar{A}_{16} & A_{66}\end{vmatrix}(\underline{D}\lambda^2t^2+\underline{N}_x^*)/2$$
$$=\begin{vmatrix}\langle A_{11}\rangle & A_{11}\\ \langle A_{16}\rangle & A_{16}\end{vmatrix}(S-N_{xy}^*)+\begin{vmatrix}\langle A_{11}\rangle & A_{11} & A_{66}\\ \langle A_{12}\rangle & A_{12} & A_{26}\\ \langle A_{16}\rangle & A_{16} & A_{66}\end{vmatrix}\beta \quad (36)$$

The three eqns (34)–(36) involve five mechanical load parameters κ, λ, μ, S, β and the thermal forces $\underline{N}_x^*$, $\bar{N}_x^*$ and N_{xy}^*. The parameters λ and μ may be easily solved from the last two of the three equations since these equations depend linearly on $(\lambda t)^2$ and $(\mu t)^2$. Substituting the solution for λ and μ into eqn (34), we obtain a single characteristic equation for the three in-plane load parameters S, β and $P = D\kappa^2t^2$ and the thermal forces $\underline{N}_x^*$, $\bar{N}_x^*$ and N_{xy}^*. Any combination of these mechanical and thermal load parameters that satisfies the characteristic equation and that yields positive values of $(\lambda t)^2$ and $(\mu t)^2$ from eqns (35) and (36) corresponds to a bifurcation state of the delamination model.

It is noteworthy that the temperature load $T(z)$ affects the buckling of the delamination model through the three thermal forces $\underline{N}_x^*$, $\bar{N}_x^*$ and N_{xy}^* only and that N_{xy}^* and S affect the bifurcation states through the combinations $S-N_{xy}^*$ only.

5. RESULTS FOR DELAMINATED HOMOGENEOUS PLATES

It is easily seen that $\langle A_{ij}\rangle = 0$ for homogeneous plates and, more generally, for delamination models with recurrent structure, where each sublaminate is configured by repeating the same generic ply group a number of times (Yin, 1986). Then eqn (36) reduces to

$$(H/2)\bar{D}\mu^2t^2-(h/2)\underline{D}\lambda^2t^2 = (h/2)\underline{N}_x^*-(H/2)\bar{N}_x^* \quad (37)$$

so that the characteristic equation becomes independent of the parameters N_{xy}^*, S and β and yields a simple relation between the axial buckling load and the right-hand side of eqn (37).

In a homogeneous isotropic or anisotropic delaminated plate there is no bending–extension coupling and eqn (34) reduces to

$$\kappa a\,\mathrm{ctn}\,\kappa b+(H/t)^3\lambda a\,\mathrm{ctn}\,\lambda a+(h/t)^3\mu a\,\mathrm{ctn}\,\mu a+3(hH/t^2) = 0 \quad (38)$$

Solutions of the system of eqns (35), (37) and (38) are computed for delamination models with the thickness ratios $h/t = 0.25$ and 0.1. For simplicity, we assume that the temperature varies linearly across the thickness of the model. Then eqn (37) reduces to

$$(\mu h)^2-(\lambda H)^2 = 6(1+\nu)\alpha(T_u-T_l) \tag{39}$$

where ν is the Poisson's ratio, α is the isotropic thermal expansion coefficient and T_u and T_l denote, respectively, the temperature on the upper and lower surfaces of the plate. Since the temperature field enters the system of eqns (35), (38) and (39) only through T_u-T_l, a uniform temperature load has no effect on the buckling solution of a delaminated homogeneous (anisotropic) plate, although it generally affects buckling of a delaminated laminate.

For several length ratios a/L, the combinations of the temperature gradient and the axial load associated with the states of bifurcation are shown in Figs 2 and 3. The horizontal coordinate $\mathscr{P}$ of the figures is the axial compression load P normalized with respect to the Euler buckling load of a perfect beam-plate without a delamination.

$$\mathscr{P} \equiv P(L/t)^2/(\pi^2 D)$$

It is clear from these figures that the temperature gradient has a very significant effect upon the critical axial load. A relatively large thermal strain caused by a high temperature in the upper region of the laminate (which contains the delamination) may cause a significant reduction in the axial buckling load. Consider a laminate with $\nu = 0.3$, $\alpha = 10\times 10^{-6}/°\mathrm{K}$ and $L/t = 30$. A temperature difference $T_u-T_l = 100°\mathrm{K}$ between the upper and lower surfaces of the laminate yields

$$\alpha(T_u-T_l)(L/t)^2 = 0.9$$

This may cause a drastic reduction in the critical axial load, as shown by the results of the figures (the amount of reduction in $\mathscr{P}$ is more than 0.5).

In previous works on buckling of delamination models under purely mechanical loads (Yin and Fei, 1984; Yin, 1989), it was shown that, depending on the relative slenderness

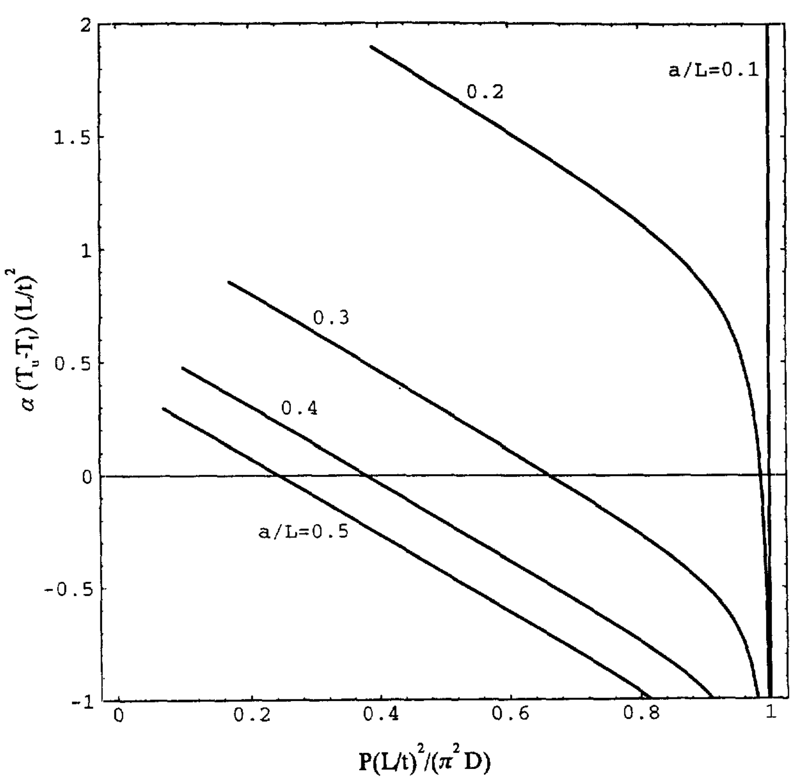

Fig. 2. Bifurcation loads of homogeneous isotropic delamination models with $h/t = 0.25$.

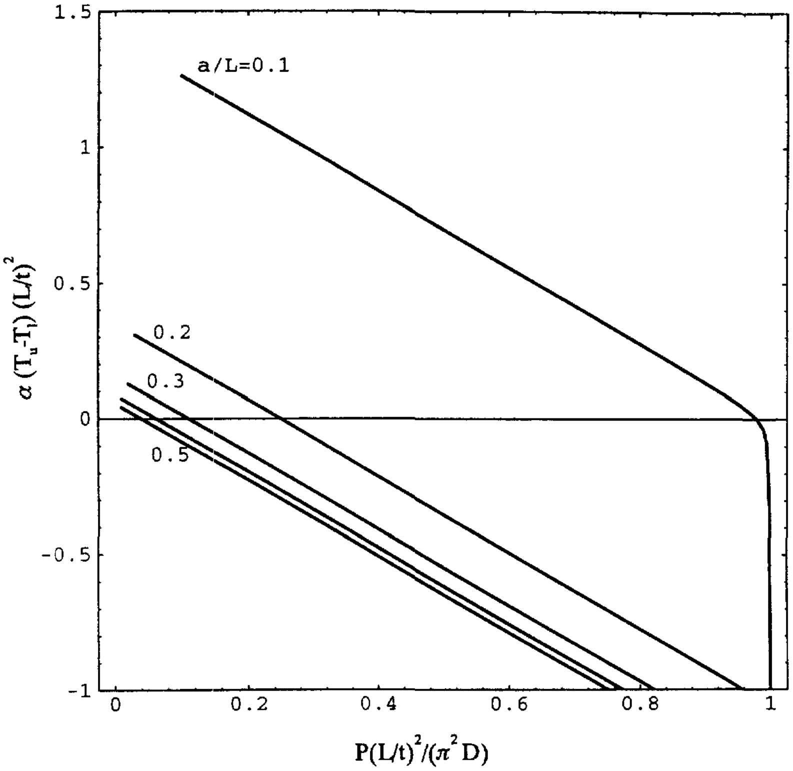

Fig. 3. Bifurcation loads of homogeneous isotropic delamination models with $h/t = 0.10$.

ratio of the upper disbonded sublaminate vs the entire laminate, the buckling behavior may be asymptotic to either a local buckling mode for the upper sublaminate or a global buckling mode for the entire model. In the local buckling mode, which is asymptotically valid in the case of a relatively thin and long upper disbonded sublaminate, the bending deformation and nonuniformity of in-plane deformation are insignificant in the base plate, so that the two ends of the upper sublaminate have negligible deflection and slope in the buckled state. Hence the bifurcation load for the local buckling mode may be closely estimated by considering buckling of the upper disbonded sublaminate (with the two ends $x = \pm a$ assumed to have negligibly small rotations) under axial shortening as induced by uniform axial compression of the base laminate, i.e.

$$\bar{P}_{cr} \approx \bar{D}(\pi t/a)^2, \quad P_{cr} = (t/h)\bar{P}_{cr} \tag{40a, b}$$

In the present case, which includes a nonuniform temperature load, the approximation of eqn (40a) remains valid for relatively thin and long delaminations, but eqn (40b) must be modified because the right-hand side of eqn (39) does not vanish. Solution of eqns (35), (39) and (40a) yields

$$\mathscr{P} + (6/\pi^2)(H/t)(1+\nu)\alpha(T_u - T_l)(L/t)^2 \approx (hL/ta)^2 \tag{41}$$

Hence the curves in Figs 2 and 3 are asymptotic to straight lines with the slope $-(t/H)\pi^2/\{6(1+\nu)\}$. This slope is independent of the length ratio a/L, and its inverse is a measure of the sensitivity of the dependence of the normalized axial buckling load to the differential thermal expansion of the top and bottom surfaces of the laminate. The curves in the figures terminate at the left-end points which correspond to $\underline{P}_{cr} = P_{cr} - \bar{P}_{cr} = 0$.

In the case of a relatively short and thick delamination, the approximate relation of eqn (41) is not valid and the buckling behavior approximates the Euler buckling of a perfect laminate without delamination. For such delamination models all curves in Figs 2 and 3 approach the vertical asymptote $\mathscr{P} = 1$ as the temperature gradient assumes large negative values. In Fig. 3, the curve corresponding to $h/t = 0.1$ and $a/L = 0.1$ shows rapid transition from the asymptotic local buckling behavior of eqn (41) to the asymptotic global buckling behavior. The transition is more gradual for the curve corresponding to $a/L = 0.2$ in Fig. 2 (where $h/t = 0.25$).

6. RESULTS FOR MULTILAYERED ANISOTROPIC DELAMINATION MODELS

For laminated delamination models $\langle A_{ij} \rangle \equiv (\bar{A}_{ij}H - \underline{A}_{ij}h)/2t$ generally does not vanish so that the in-plane shearing force S and the transverse in-plane strain β affect buckling according to eqn (36). However, since the present study is concerned mainly with the thermal effects on buckling, the following solutions are presented for the case $S = \beta = 0$.

We consider eight-layer symmetric angle-ply laminates with the stacking sequence $[(45/-45)_2]_s$ and with a strip delamination in the second interface from the top surface. If the layers are made of unidirectional AS/3501 graphite/epoxy composite with orthotropic elastic and thermal coefficients $E_1 = 138$ GPa, $E_2 = 8.96$ GPa, $G_{12} = 7.1$ GPa, $\nu_{12} = \nu_{23} = 0.3$, $\alpha_1 = -0.3 \times 10^{-6}/°K$ and $\alpha_2 = 28.1 \times 10^{-6}/°K$ (see Table 1.7 and 8.3 in Tsai and Hahn, 1980), the buckling loads for various delamination lengths are shown in Fig. 4. The results are qualitatively similar to those of Fig. 2 for the isotropic delaminated plate with the same thickness ratio, $h/t = 0.25$. However, the coupling stiffnesses $[\underline{B}_{ij}]$ and $[\bar{B}_{ij}]$ associated with the anisotropic disbonded sublaminates affect the characteristic equation [eqn (34)] so that, when the thermal load is absent, the bifurcation loads of Fig. 4 are significantly smaller than those shown in Fig. 2. Furthermore, because of the small value of α_1, the asymptotic slope of the curves in Fig. 4 are several times greater than that of Fig. 2. Hence the buckling loads are less sensitively affected by the imposed temperature gradient.

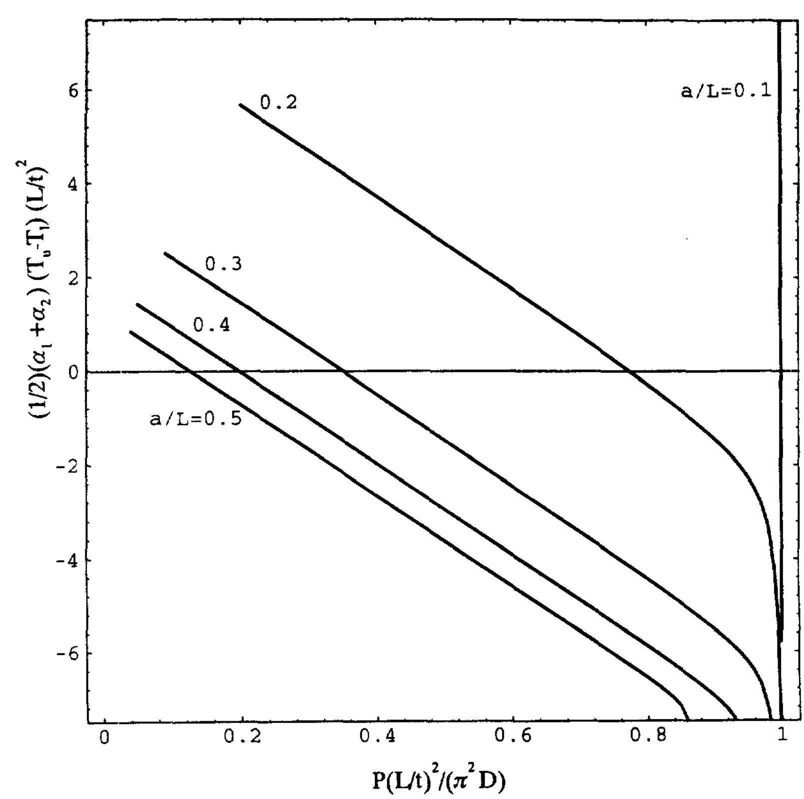

Fig. 4. Results for delaminated $[(45/-45)_2]_s$ AS3501 graphite/epoxy laminates, $h/t = 0.25$.

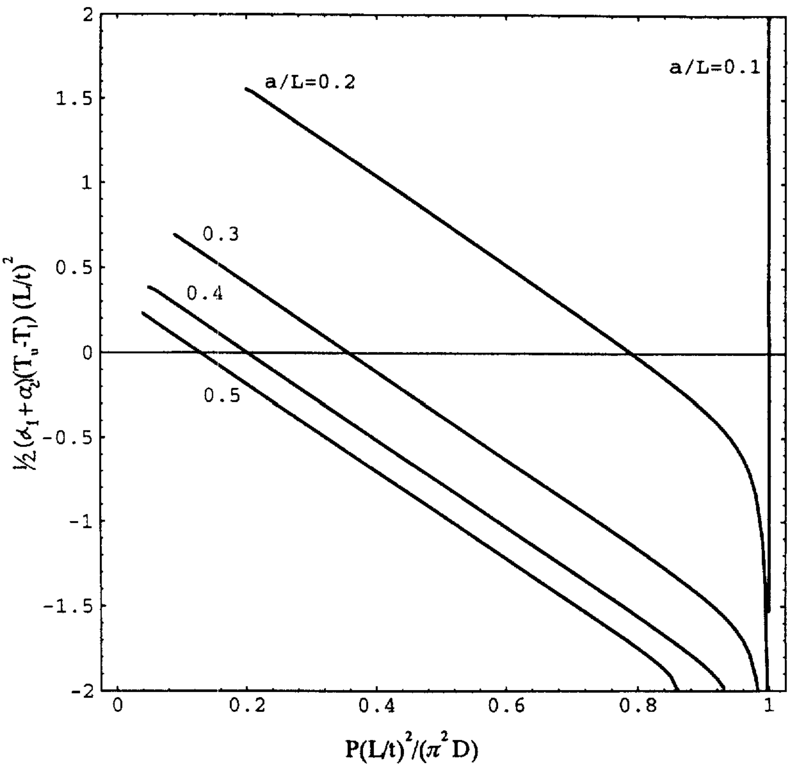

Fig. 5. Results for delaminated $[(45/-45)_2]_s$B(4)/5505 boron/epoxy laminates, $h/t = 0.25$.

The results of an identical delamination model made of B(4)/5505 boron/epoxy composite are shown in Fig. 5. The layers have the orthotropic properties $E_1 = 204$ GPa, $E_2 = 18.5$ GPa, $G_{12} = 5.59$ GPa, $\nu_{12} = \nu_{23} = 0.23$, $\alpha_1 = 6.1 \times 10^{-6}/°K$ and $\alpha_2 = 30.3 \times 10^{-6}/°K$. The curves in Fig. 5 have a much smaller asymptotic slope compared to those of Fig. 4, implying significantly greater effects of temperature gradients upon the buckling load.

7. SUMMARY AND CONCLUDING REMARKS

Under the assumption of generalized plane deformation (i.e. all strain components are independent of y), an exact buckling analysis is presented for a multilayered strip delamination model subjected to a temperature load that may vary arbitrarily in the thickness direction. The analysis is based on the thermoelastic constitutive equations of anisotropic laminates, i.e. classical laminated plate theory is applied to the intact and disbonded sublaminates, and the anisotropic elastic constants and thermal expansion coefficients of the constituent plies are assumed to be absolute constants unaffected by temperature increase. Under these assumptions, the temperature load affects the buckling behavior of a strip delamination model through the axial thermal forces $\underline{N}_x^*$ and $\bar{N}_x^*$ of the disbonded sublaminates and the shearing thermal force N_{xy}^* of the intact laminate. The bifurcation states are characterized by those combinations of the thermal and mechanical load parameters $\underline{N}_x^*$, $\bar{N}_x^*$, $S - N_{xy}^*$, P $(\equiv D\kappa^2 t^2)$ and β $(\equiv \varepsilon_y)$ which satisfy a characteristic equation. The characteristic equation, obtained by eliminating the parameters λ and μ from the three algebraic eqns (34)–(36), reveals explicitly how the various geometrical, material and load parameters affect the buckling behavior of the delaminated plate. If the laminate is homogeneous and isotropic and if the temperature varies linearly in the thickness direction, then the characteristic equation reduces to a relation between the axial buckling load and the differential thermal strain of the upper and lower surfaces, and the only parameters involved in this relation are the ratios among h, t, a, L and the Poisson's ratio of the material.

Bending–stretching coupling stiffness matrices $[\underline{B}_{ij}]$ and $[\bar{B}_{ij}]$ associated with unsymmetric disbonded sublaminates may significantly reduce the buckling load through their contributions to eqn (34). The coupling effects also cause the axial and shearing components of the membrane strains in the buckled sublaminates to vary sinusoidally with the axial coordinate x, even though the axial force and the in-plane shearing force are constant in each sublaminate. The transverse in-plane strain ε_y ($\equiv \beta$) and the in-plane shearing force S generally affect buckling, as indicated by eqn (36).

A temperature gradient corresponding to a moderate differential thermal expansion of the upper and lower surfaces of the laminate may drastically change the axial buckling load of the delamination model. If $(h/a)/(t/L)$ is smaller than unity by a certain margin (i.e. if the upper disbonded sublaminate is more slender than the whole laminate) so that bifurcation is initiated by local buckling of the upper sublaminate, then the dependence of the buckling load upon the temperature gradient is asymptotic to a linear relation. For homogeneous delamination models the slope of this linear relation is *independent* of the normalized delamination length, a/L. This slope, whose inverse is a measure of the sensitivity of the axial buckling load to the imposed temperature gradient, may be calculated from eqn (36) by using the asymptotic relation of eqn (40a).

Moisture concentration produces additional strain in a manner analogous to the generation of thermal strain by the temperature field. Hence the preceding formulation and analysis of the thermal effects on buckling may also be used to evaluate the similar effects of a moisture gradient when appropriate substitutions are made for the variables and the expansion coefficients.

While the present analysis was based on the classical laminate theory for the sake of simplicity, it may be modified to account for the thickness shear effect by including additional kinematical variables and out-of-plane shearing forces [see Kardomateas and Schmueser (1988) and Chen (1991) for the results under purely mechanical loading]. Finally, fiber composites at increased temperature may show loss of stiffness in the direction transverse to the fibers, so that the elastic moduli are temperature dependent rather than absolute constants. Such softening effect may cause further reduction in the buckling load under temperature influence. The effect may be assessed in the present scheme of analysis by using elastic moduli appropriate to the temperature load.

REFERENCES

Chai, H. (1990) Three-dimensional fracture analysis of thin film debonding. *International Journal of Fracture* **46,** 237–256.

Chen, H. P. (1991) Shear deformation theory for compressive delamination buckling and growth. *AIAA Journal* **29,** 813–819.

Cochelin, B. and Potier-Ferry, M. (1991) A numerical model for buckling and growth of delaminations in composite laminates. *Computer Methods in Applied Mechanics and Engineering* **89,** 361–380.

Garg, A. C. (1988) Delamination—a damage mode in composite structures. *Engineering Fracture Mechanics* **29,** 557–584.

Hutchinson, J. W and Suo, Z. (1992) Mixed mode cracking in layered materials. In *Advances in Applied Mechanics,* ed. J. W. Hutchinson and T. Y. Wu, Vol. 29, pp. 63–191. Academic Press, San Diego.

Kardomateas, G. A. and Schmueser, D. W. (1988) Buckling and postbuckling of delaminated composites under compressive loads including transverse shear effects. *AIAA Journal* **26,** 337–343.

Larsson, P. L. (1991) On multiple delamination buckling and growth in composite plates. *International Journal of Solids and Structures* **27,** 1623–1637.

Lee, J., Gurdal, Z. and Griffin, O. H. Jr (1993) Layer-wise approach for the bifurcation problem in laminated composites with delaminations. *AIAA Journal* **31,** 331–338.

Peck, S. O. and Springer, G. S. (1991) The behavior of delaminations in composite plates—analytical and experimental results. *Journal of Composite Materials* **25,** 907–929.

Simitses, G. J., Sallam, S. and Yin, W.-L. (1985) Effect of delamination of axially loaded homogeneous laminated plates. *AIAA Journal* **23,** 1437–1444.

Storakers, B. (1989) Nonlinear aspects of delamination in structural members. In *Theoretical Mechanics, Proceedings in International Congress on Theoretical and Applied Mechanics,* ed. P. Germain, M. Piau and D. Caillerie, pp. 315–336. Elsevier, New York.

Tsai, S. W. and Hahn, H. T. (1980) *Introduction to Composite Materials.* Technomic, Westport, CT.

Wang, S. S., Zahlan, N. M. and Suemasu, H. (1985) Compressive stability of delaminated random short-fiber composites. Part I—Modeling and methods of analysis; Part II—Experimental and analytical results. *Journal of Composite Materials* **19,** 296–316, 317–333.

Whitcomb, J. D. (1989) Three-dimensional analysis of a postbuckled embedded delamination. *Journal of Composite Materials* **23,** 862–889.

Yin, W.-L. (1986) Cylindrical buckling of laminated and delaminated plates. *Proceedings of the AIAA/ASME/ASCE/AHS 27th SDM Conference*, San Antonio, TX, pp. 165–179.

Yin, W.-L. (1989) Recent analytical results in delamination buckling and growth. In *Interlaminar Fracture in Composites*, ed. E. A. Armanios, pp. 253–266, Trans Tech, Switzerland.

Yin, W.-L. and Jane, K.-C. (1992) Refined buckling and postbuckling analysis of two-dimensional delaminations—I. Analysis and validation; II. Results for anisotropic laminates and conclusion. *International Journal of Solids and Structures* **29,** 591–610, 611–639.

Yin, W.-L. and Fei, Z. (1984) Buckling load of a circular plate with a concentric delamination. *Mechanical Research Communications* **11,** 337–344.

Yin, W.-L. and Fei, Z. (1988) Delamination buckling and growth in a clamped circular plate. *AIAA Journal* **26,** 438–445.

Yin, W.-L., Sallam, S. N. and Simitses, G. (1986) Ultimate axial load capacity of a delaminated beam-plate. *AIAA Journal* **24,** 123–128.